ISSN 1009-3095 *Journal of Zhejiang University SCIENCE* V.4, No.2, P.175-180, Mar.-Apr., 2003
http://www.periodicals.com.cn; http://www.zju.edu.cn/English
http://www.zjupress.com; http://lib.zju.edu.cn/eindex.htm; jzus@zju.edu.cn

Large eddy simulation of a particle-laden turbulent plane jet[※]

JIN Han-hui(金晗辉), LUO Kun(罗坤), FAN Jian-ren(樊建人)[†]
CEN Ke-fa(岑可法)

(*Department of Energy Engineering, Zhejiang University, Hangzhou 310027, China*)

[†]E-mail: fanjr@mail.hz.zj.cn

Received Jan.29, 2002; revision accepted May 10, 2002

Abstract: Gas-solid two-phase turbulent plane jet is applied to many natural situations and in engineering systems. To predict the particle dispersion in the gas jet is of great importance in industrial applications and in the designing of engineering systems. A large eddy simulation of the two-phase plane jet was conducted to investigate the particle dispersion patterns. The particles with Stokes numbers equal to 0.0028, 0.3, 2.5, 28 (corresponding to particle diameter 1 μm, 10 μm, 30 μm, 100 μm, respectively) in *Re* = 11 300 gas flow were studied. The simulation results of gas phase motion agreed well with previous experimental results. And the simulation results of the solid particles motion showed that particles with different Stokes number have different spatial dispersion; and that particles with intermediate Stokes number have the largest dispersion ratio.

Key words: Large eddy simulation, Particle dispersion, Gas-solid two-phase plane jet
Document code: A **CLC number:** TK16

INTRODUCTION

Many experimental and numerical studies have been completed to investigate the particle motion in turbulence. Previous fluid dynamics studies were commonly based on time-averaged Reynolds equations, such as the two-equation model. Just like the carrier gas phase, the particle phase may also have its own fluctuation velocity caused by time-dependent carrier gas flow velocity or by particle-particle collision. A series of models were developed to determine the motion of the particles in gas flow. The particle-source-in cell (PSI-CELL) model (Crowe et al., 1977) was applied to represent the particle field by particle trajectories. In this model, the particle trajectory was obtained from integrating the particle's motion equation; and the particle mass and velocity were calculated along the trajectory simultaneously. Cen et al. (1989) and Zha et al.(2000) introduced a fluctuation-spectrum-random-trajectory (FSRT) model to simulate the particle motion, assuming a predefined spectrum function to select the fluctuation velocity. In these models, the flow field was reconstructed from the mean flow quantities. Because the time-averaged fluid models could not predict anisotropic turbulence precisely, it is difficult to investigate the particle motion in anisotropic turbulence although many other models had been developed previously.

It is believable that the particle dispersion is mainly influenced by the organized large-scale turbulent structures of the carrier gas phase at each time. More and more recent experimental and numerical investigations focused on the importance of the large eddy structure in particle dispersion. Wen et al. (1992) experimentally and numerically investigated particle dispersion by large eddy structure in a plane temporal mixing layer. Similar investigations by Ling et al. (1998), Fan et al.(2001) and Zheng (2001) with direct numerical simulation (DNS) showed that the Stokes number of the particles played an important role in particle dispersion patterns. For mixing layers, the large scale eddy dynamics are dominated by pairing interaction between eddy structures of the same sign. For plane jet,

---

[※] Project (No. G19990222) supported by the Special Funds for Major State Basic Research of China

[†] Author for correspondence

there would be pairs of reversed eddy structures because of the existence of the two opposite free shear boundaries of the plane jet. Therefore, particle dispersion in plane jet may differ from that in plane mixing layer and may be more complex. Furthermore, numerical studies such as DNS are limited to low Reynolds number flows because of the difficulties in meeting the conditions of DNS or other numerical methods needed. For engineering systems where flows are of high Reynolds number usually, large eddy simulation (LES) may be a more efficient way because it can be applied to the simulation of high-Reynolds turbulence. LES incorporates the advantages of both DNS and RANS (Reynolds-averaged Navier-Stokes) models, to simulate large eddy directly and to simulate small eddy with models. Wang (1998) studied particle mean-square dispersion in the viscous sublayer, buffer layer, or logarithmic region of a channel flow. Uijttewaal et al. (1996) studied the various mechanisms of particle motion and deposition between particles of large range of relaxation times. But few numerical simulations of particle dispersion and the large eddy structures in a plane jet are reported.

The present investigation aims to examine the dispersion of particles with different Stokes numbers in plane jet flow at *Re* = 11300 by large eddy simulation when gravitation influence is neglected.

MATHEMATICAL MODEL

1. The flow configuration

The flow configuration of plane jet is shown in Fig. 1. The flow is described in a Cartesian coordinate system (x, y) in which x axis is aligned with the inlet jet direction, and y axis is perpendicular to x. A fixed two-dimensional plane jet with $2H$ = 20 mm and the constant stream velocity U_0 = 10 m/s of the two phases is presented. We assume that the gas flow is incompressible and that the fluid properties are constant. The Reynolds number is defined as $Re = U_0 \cdot 2H/v$. All geometrical lengths are scaled with H. The material density of the particle phase is $\rho_q = 1 \times 10^3$ kg/m^3. The diameters of the particles are 1 μm, 10 μm, 30 μm, 100 μm respectively, and the corresponding Stokes number St = 0.0028, 0.3, 2.5, 28. Number density of the particle is $1 \times 10^7/\text{m}^3$.

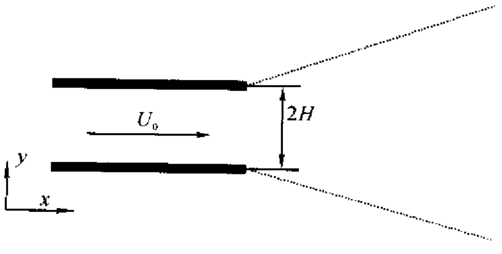

Fig.1 Flow configuration of the plane jet

The two-dimensional numerical models is described below.

2. Governing equations of the gas phase

Here the LES of volume averaged approach is used to solve the time-dependent Navier-Stokes (N-S) equations, and the most well-known sub-grid scale (SGS) model introduced by Smagorinsky (1963) is adopted.

Assume the volume-averaged variance can be described as follows:

$$\bar{\phi}(x, y, t) = \frac{1}{\Delta x \cdot \Delta y} \cdot \int_{x-\frac{1}{2}\Delta x}^{x+\frac{1}{2}\Delta x} \int_{y-\frac{1}{2}\Delta y}^{y+\frac{1}{2}\Delta y} \phi(\xi, \eta, t) \mathrm{d}\xi \mathrm{d}\eta .$$

Then volume-averaged two-dimensional N-S equations can be written as follows:

$$\frac{\partial u_i}{\partial t} = \frac{\partial}{\partial x_j}[\bar{u}_i \bar{u}_j] - \frac{\partial}{\partial x_i}\left[\frac{p}{\rho}\right] + \frac{\partial}{\partial x_j}\left[\nu\left(\frac{\partial u_i}{\partial x_j} + \frac{\partial u_j}{\partial x_i}\right) + T_{ij}\right],$$

where SGS tensor T_{ij}: $T_{ij} = u_i u_j - \overline{u_i u_j}$. An eddy-viscosity assumption (Boussinesq's hypothesis) is used to model the SGS tensor:

$$T_{ij} = 2\gamma_t S_{ij} + \frac{1}{3} T_{\text{LL}} \delta_{ij},$$

where $S_{ij} = \frac{1}{2}\left(\frac{\partial \bar{u}_i}{\partial x_j} + \frac{\partial \bar{u}_j}{\partial x_i}\right)$, $\gamma_t = (C_s \Delta)^2 |S|$, $|S| = (2 S_{ij} S_{ij})^{\frac{1}{2}}$, $\Delta = (\Delta x \cdot \Delta y)^{\frac{1}{2}}$.

The two-dimensional N-S equations can be described as follows.

Continuum equation:

$$\frac{\partial}{\partial x}(\rho\bar{u})+\frac{\partial}{\partial r}(\rho\bar{v})=0$$

Momentum equation:

$$\frac{\partial u_i}{\partial t}=-\frac{\partial}{\partial x_j}[\bar{u}_i\ \bar{u}_j]-\frac{\partial}{\partial x_i}\left[\frac{\bar{p}}{\rho}\right]+\frac{\partial}{\partial x_j}\left[(\gamma+\gamma_t)\left(\frac{\partial u_i}{\partial x_j}+\frac{\partial u_j}{\partial x_i}\right)\right],$$

where $C_s = 0.15$ is used in the present work.

3. Governing equation of the particle phase

Since the density ratio $\rho_p/\rho > 1000$, the Basset force, the added force, can be neglected. And the collisions between the particles can be ignored because of low particle loading. The Magnus force is neglected due to the small gradient of the velocity. In addition, the Saffman force should be considered only when the particle rotation is very high, so it is neglected here too. Meanwhile, gravitation of the particle is ignored. Therefore only the drag force is taken into consideration to study the particle dispersion. Then the equation of the particle motion is given below:

$$\frac{dU_p}{dt}=\frac{f}{\tau_A}(U-U_p),$$

where $\tau_A = \dfrac{\rho_p d_p^2}{18\mu}$,

$$f = 1 + 0.15Re_p^{0.687},$$

$$Re_p = \frac{|U-U_p|d_p}{\gamma}.$$

4. Simulation method for the gas phase

A two dimensional finite volume incompressible code based on a $X \times Y = 352 \times 481$ staggered grid arrangement is used. The implicit difference scheme in time and the second-order Crank-Nicolson scheme are used. The span of the computational domain covers $X \times Y = 96H \times 68H$. Full developed boundary conditions at the outlet and static surrounding environment conditions are assumed.

RESULTS AND DISCUSSION

The numerical results of time-averaged streamwise velocity profiles at the cross sections of $x/H = 8, 16, 24$ compared with the experimental results (Reichardt, 1951) are shown in Fig. 2, where u_m is the streamwise velocity on the centerline of the nozzle, y_u is the distance between the position where the streamwise velocity $u/u_m = 0.5$ and the centerline of the jet. The agreement between the numerical results and the empirical results is quite good in these cross sections except for the little disagreement due to the numerical calculation of limited time period ($t = 320T$, where T is the scalar time defined as $T = H/U_0$). The self-organizing flow mechanism in a plane jet can be easily obtained. Fig.3 (a) – Fig.3(d) show the contour of the spatial extended vorticity of the plane jet developing with increasing time. The producing, shedding, pairing and emerging of the eddies can be clearly observed.

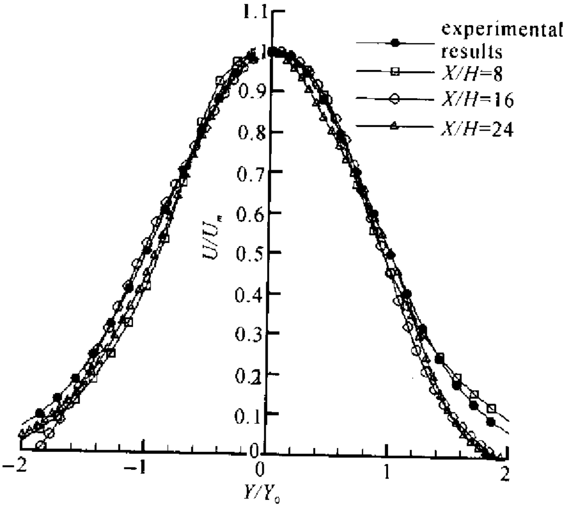

Fig.2 Self-organization of the streamwise velocity

Figs. 4 – 7 show the spatial distribution of the particles with Stokes number equal to 0.0028, 0.3, 2.5, 28 respectively in the flow field at $t = 480T$. The difference between the particles of different Stokes number is obvious.

The particles at $St = 0.0028$ (Fig.4) follow the gas flow compactly, the entangling process of the surrounding gas into the jet and the eddy pairing process can be observed easily according to the spatial distribution of the particles. Because of the good ability to trace the gas flow, particles at low Stokes number are often applied as tracer of flow field in experiments. Particles at the $St = 28$ (Fig.7) display a significant dif-

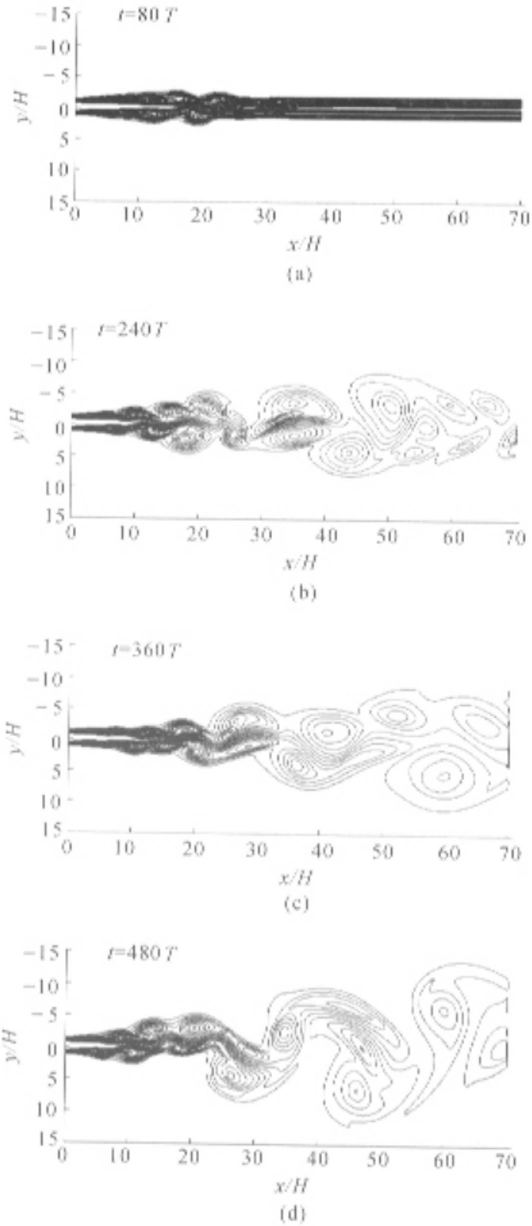

Fig.3 Spatial vorticity of gas stream
(a) $t = 80\,T$; (b) $t = 240\,T$; (c) $t = 360\,T$; (d) $t = 480\,T$

ference in spatial dispersion pattern from those observed at $St = 0.0028$. The particle distribution varies a little from the inlet to the outlet, where a small wave is produced by the large scale eddy structures of the gas flow. The most interesting spatial distribution map of particles appears at mediate Stokes number such as $St = 2.5$ (Fig.6). The particles concentrate densely near the outer boundary of the large scale eddy structures and have nearly zero concentration throughout the central region of the structures. The particles are stretched like a folded string around the large scale eddy structures. This tendency of the particle concentration is consistent with the DNS results of plane mixing layer (Zheng, 2001). In addition, particle accumulation in the rib or the saddle region between the adjoining eddy structures is very apparent. The $St = 0.3$ particles' spatial dispersion pattern (Fig.5) is just like those of $St = 2.5$ and $St = 0.0028$, and the extent of the concentration near the boundary of the eddy structures and distribution inside the structure of $St = 0.3$ particles is just between those of $St = 2.5$ and $St = 0.0028$ particles.

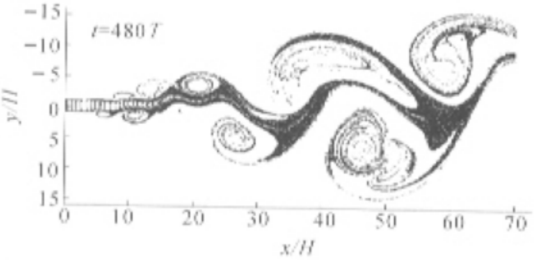

Fig.4 Spatial distribution of $St = 0.0028$ particles

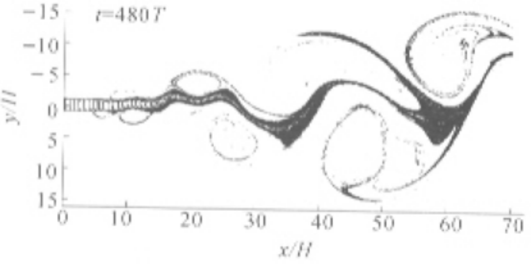

Fig.5 Spatial distribution of $St = 0.3$ particles

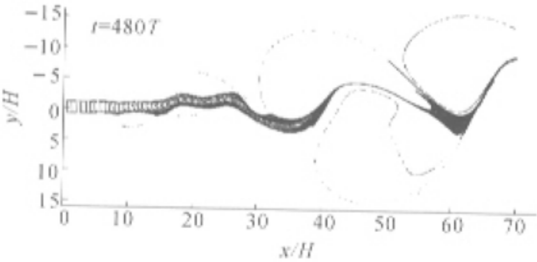

Fig.6 Spatial distribution of $St = 2.5$ particles

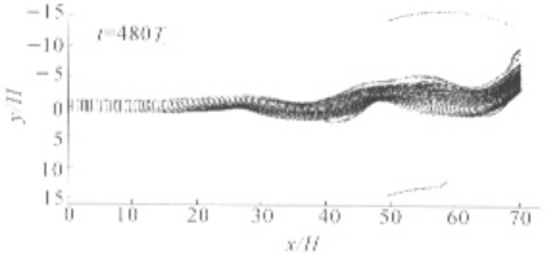

Fig.7 **Spatial distribution of *St* = 28 particles**

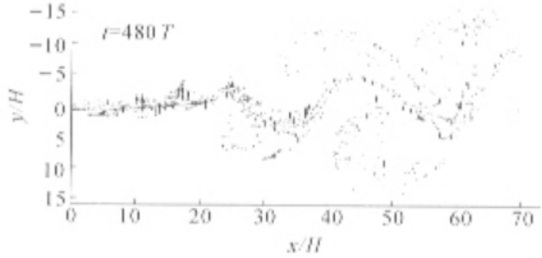

Fig.8 **Relative velocity vectors of particles (*St* = 0.0028)**

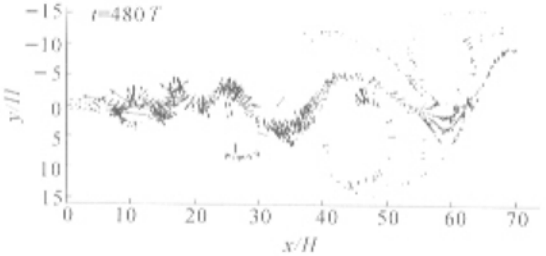

Fig.9 **Relative velocity vectors of particles (*St* = 0.3)**

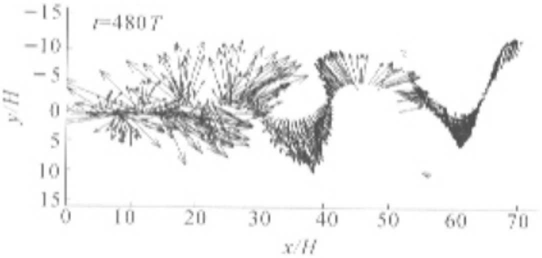

Fig.10 **Relative velocity vectors of particles (*St* = 2.5)**

To illustrate the particle motion associated with the local eddy structure, Figs. 8 – 10 show the particles' relative velocity vectors where the local gas stream velocity has been subtracted from the particle velocity at the moment of $t = 480T$. The particles at $St = 0.0028$ (Fig. 8) show nearly zero velocity relative to the gas stream. The particles at $St = 0.3$ (Fig. 9) show small relative velocity in both streamwise direction and radial direction of the large scale eddy structures. The particles at $St = 2.5$ (Fig. 10) show the largest relative velocity of all in radial direction of the eddy structures and not very large relative velocity in the streamwise direction. Because the trajectory of particles at $St = 28$ vary little, their relative velocity vector maps are not pictured. According to the magnitude of the relative velocity vectors above, we can also draw the conclusion that particles of mediate Stokes number have the largest dispersion in the plane jet.

The cross-stream particle dispersion ratio at different Stokes number in different time phase is shown in Fig. 11. The dispersion ratio is defined as:

$$D = \frac{\left[\sum_{1}^{N}(y_i - y_{i0})^2\right]^{\frac{1}{2}}}{N},$$

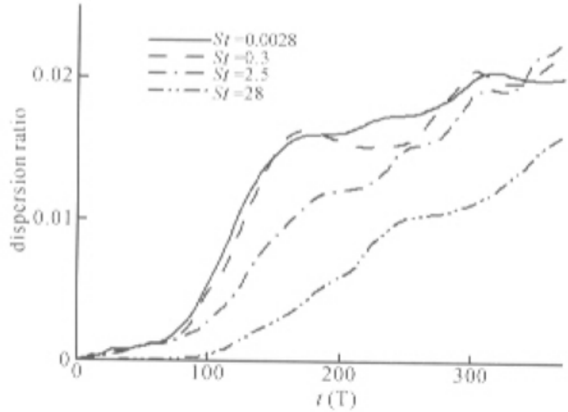

Fig.11 **Spatial dispersion ratio for different particles**

where: N is the total number of the particles considered; y_{i0} is the ith particle's initial y position and y_i is the ith particle's present y position. It can be seen that for $St = 0.0028$ particles, the dispersion ratio increases rapidly as the short relaxation time of the low stokes number particles makes them disperse quickly. And the larger the Stokes number of the particles, the slower they disperse in the flow field. But the dispersion ratio of mediate Stokes number ($St = 0.3$, 2.5) particles soon exceed that of low Stokes number. The particles of the largest Stokes number have the lowest dispersion in the flow field. These coincide with the conclusions drawn previously.

CONCLUSIONS

A 2-D large eddy simulation of gas-solid two-phase flow was completed to study the particle dispersion in plane jet. The vorticity structure resulted from LES is qualitatively similar to that from DNS and the results on gas phase agreeing well with the experimental results showed that 2D-LES can predict plane jet well and can be applied to gas-solid two phase plane jet.

The numerical results of the particle phase quantitatively showed that the extent of particle dispersion can be strongly governed by the Stokes number. The particles with large Stokes number have the lowest spatial dispersion ratio, while the dispersion ratio of the intermediate Stokes number particles is the highest of all. When particles with small Stokes number are circling with the gas flow in the large eddy structures, the particles with large Stokes number cross the eddy structures directly due to their large inertia.

References

Blümke, E., Brandt, M., Eickhoff, H. and Hassa, C., 1993. Particle dispersion in highly swirling turbulent flows. *Part. Syst. Charact*, **10**: 182 - 190.

Cen, K. F. and Fan, J. R., 1989. A numerical model for the turbulent fluctuation and diffusion of gas-particle flows and its application in the freeboard of afluidized bed. *Particle Science and Technology*, **6**(1).

Crowe, C. T., Sharma, M. P. and Stock, D. E., 1977. The Particle-Source-in-CELL (PSI-CELL) for gas-droplet flows. *J. Fluids Engr.*, **99**: 325 - 331.

Fan, J. R., Zheng, Y. Q., Luo, Z. H. and Cen, K. F., 2001. Direct simulation of particle dispersion in a three-dimensional temporal mixing layer. *Proceedings of the Royal Society of London Series A.*, **457**: 2151 - 2166.

Ling, W., Chung, J. N., Troutt, T. R. and Crowe, C. T., 1998. Direct numerical simulation of a three-dimensional temporal mixing layer with particle dispersion. *J. Fluid Mech.*, **358**: 61 - 85.

Reichardt, H., 1951. Gesetzmassigkeiten der freien turbulenz VCI forschung sheff. *ZAMM*, **30**: 414.

Smagorinsky, J., 1963. General circulation experiments with the primitive equation. *Mon. Weather Rev.*, **91**(3): 99 - 164.

Sohankar, A., Norberg, C. and Davidson, L., 1999. Simulation of unsteady three-dimensional flow around a square cylinder at modeate Reynolds number. *Phys. Fluids*, **11**(2): 99 - 165.

Uijttewaal, W. S. J. and Oliemans, R. V. A., 1996. Particle dispersion and deposition in direct numerical and large eddy simulations of vertical pipe flows. *Physics of Fluids*, **8**(10): 2590 - 2604.

Wang, Q., Squires, K. D. and Simonin, O., 1998. Large eddy simulation of turbulent gas solid flows in a vertical chnnel and evaluation of second-order models. *Int. J. Heat and Fluid Transfer*, **19**: 505 - 511.

Wen, F., Kamalu, N., Chung, J. N., Crowe, C. T. and Troutt, T. R., 1992. Particle dispersion by vortex structures in plane missing layer. *ASME J. Fluids Engr.*, **114**: 657 - 666.

Zha, X. D., Fan, J. R., Sun, P. and Cen, K. F., 2000. Numerical simulation on dense gas-particle riser flow. *Journal of Zhejiang University SCIENCE*, **1**(1): 27 - 28.

Zheng Y. Q., 2001. Direct numerical simulation and experimental verification on the turbulent coherent structures in gas-particle two-phase mixing layer. Doctor dissertation of Zhejiang University, China(in Chinese).

Zhou, Q. and Leschziner, M. A., 1996. Modelling Particle Dispersion in Anisotropic Turbulence. ECCOMAS 96. Wiley, New York, USA.

Zhou, Q. and Yao, S. C., 1992. Group modeling of impacting spray dynamics. *Int. J. Heat Mass Transf.*, **35**: 121 - 129.